Chemical Physics 127 (1988) 313–324
North-Holland, Amsterdam

ELECTRONIC STATES AND POTENTIAL ENERGY SURFACES OF GOLD AND SILVER TRIMERS

K. BALASUBRAMANIAN [1] and M.Z. LIAO [2]
Department of Chemistry, Arizona State University, Tempe, AZ 85287, USA

Received 20 May 1988

Multiconfiguration SCF (MCSCF) followed by second-order configuration interaction calculations, MCSCF/POLCI and MCSCF/MRSDCI calculations which included the d shells in the active space (33 electrons) are carried out on both Ag_3 and Au_3. The MRSDCI calculations included about 400000 configurations. In addition the effects of higher-order excitations and spin–orbit coupling are calculated using Davidson's correction and relativistic CI calculations. Three low-lying electronic states were found for both the clusters namely $^2B_2$ (isosceles triangle), $^2A_1$ (isosceles triangle) and $^2\Sigma_u^+$ (linear). The geometry of the $^2B_2$ (isosceles triangle) was found to be very sensitive to the d-correlation corrections since the $^2B_2$ surface is quite shallow near the bent minimum. The apex angles of the isosceles triangles of $^2B_2$ and $^2A_1$ were both acute.The $^2A_1$ and $^2B_2$ bent minima were found to be nearly degenerate for both Ag_3 and Au_3. The final MRSDCI $^2B_2$–$^2A_1$ separation which included spin–orbit effects is 0.16 kcal/mole for Au_3 and 0.69 kcal/mole for Ag_3, the $^2B_2$ state being the ground state of both the clusters. The equilibrium geometries predicted by POLCI calculations agree well with more accurate MRSDCI calculations. The spin–orbit coupling lowered the $^2B_2$–$^2A_1$ separation by 0.38 kcal/mole for Au_3 and 0.05 kcal/mole for Ag_3. The Mulliken population analyses and the dipole moments for the two clusters reveal that both the clusters are ionic (Au_3 being more ionic) and the apex atom of the isosceles triangle carries the positive charge for the $^2B_2$ state and negative charge for the $^2A_1$ state. The gross d and p populations of the metal atom are larger for silver in comparison to gold, while the s populations are larger for gold in comparison to silver.

1. Introduction

The electronic properties of silver and gold clusters are of considerable interest since these clusters not only have catalytic properties but also are models of surfaces and thin films of gold and silver. In addition, the silver clusters are of importance in photographic processes. The fundamental interest in these clusters stems from the intriguing dramatic contrast between the bonding in silver and gold. It is now well documented that gold dimer forms a stable bond in comparison to silver dimer contrary to the common sense expectation. The general area of transition metal clusters has been reviewed recently [1–3].

There are a few experimental gas phase and matrix spectroscopic studies on both Ag_3 and Au_3. The Raman spectroscopic investigation of Schulze et al. [4] seems to suggest a linear structure for Ag_3 in accordance with a single Raman band at 120.5 cm^{-1} although the reliability of their results have been questioned [5]. Ozin and co-workers [6,7] have measured the UV–visible spectra of Ag_{1-3}/Ar, Xe inert gas mixtures generated by condensing silver atoms with the rare gas mixtures at 12 K and irradiating the deposits at the frequencies of silver atomic resonance absorption lines. From these spectra, they have considered that there are "photoisomerization" processes which can be deduced for an Ag_3 $D_{\infty h}$ linear to C_{2v} nonlinear to D_{3h} triangular structure interconversions. Thus, it is postulated that there are nearly degenerate states for Ag_3 with equilateral triangular $1a_1'^2 1e'^1$ (D_{3h}) or isosceles $1a_1^2 1b_2^1$ and $1a_1^2 2a_1^1$ C_{2v} forms. Hilpert and Gingerich [8] have obtained the atomization energies of Ag_3 to be 2.63 eV corresponding to a linear geometry and 2.54 eV for the bent geometry using the thermodynamic third law calculations deduced from high temperature mass spec-

[1] Alfred P. Sloan Fellow; Camille and Henry Dreyfus Teacher–Scholar.
[2] Present address: Department of Chemistry, Tsinghua University, Beijing, PR China.

trometry with a Knudson cell. The small difference in the atomization energies of linear and bent structures also seems to suggest that there are nearly degenerate states for Ag_3. Howard and co-workers [9,10] have obtained the first positive EPR identification of a neutral silver cluster Ag_3 and suggested that Ag_3 is probably bent with a $^2B_2$ (C_{2v}) ground state.

A few authors have carried out semi-empirical theoretical calculations on Ag_3. Baetzold [11,12] assumed the linear structure as the ground state of Ag_3 in the calculations of larger Ag clusters including up to 30 atoms with extended Hückel and complete neglect of differential overlap (CNDO) methods. Richtsmeier and co-workers [13,14] predicted that the linear structure of Ag_3 is close in energy to the acute bent structure with the semi-empirical diatomics-in-molecules (DIM) method. Basch [15] carried out ab initio effective core potential SCF/CI calculations for Ag_3. However, these calculations were carried out at a fixed Ag–Ag bond length. The optimization of the Ag–Ag bond length for all angles appears to be important. Walch et al. [36] have carried out single configuration SCF/CI calculations on selected regions of the potential energy surfaces of Ag_3. They found two nearly degenerate bent states for Ag_3. In the present investigation superior CASSCF/MRSDCI calculations including spin–orbit coupling for both Ag_3 and Au_3 are carried out.

The related gold and silver dimers have been investigated by Pitzer and co-workers [16,17]. Pitzer and co-workers showed that relativistic mass–velocity corrections shrink the outer 6s orbital of the gold atom leading to a shorter and stable Au–Au bond in comparison to the Ag–Ag bond. The only ab initio investigation on Au_3 is the one by Balasubramanian and Liao [18] who carried out CASSCF/SOCI calculations on the $^2B_2$ and $^2A_1$ states without d correlations. The effect of d correlation was addressed on Au_2 but the impact of d correlation on the geometries of the electronic states of Au_3 and the energy separations has not been addressed to date. In addition the importance of spin–orbit effects on the electronic states of both silver and gold trimers have not been studied at all. Theoretical studies of electronic properties of molecules containing very heavy atoms is a topic of considerable activities in recent years [19–27].

The objectives of the present investigation are (i) to carry out large-scale configuration interaction calculations which include all the 33 electrons using the CASSCF/MRSDCI methodology (ii) to calculate the entire bending potential energy surfaces of the two clusters including d correlation effects and (iii) to calculate accurately the spin–orbit effects using the recently developed relativistic configuration interaction method for polyatomics. Such calculations are carried out on Au_3, Ag_3, Au_2 and Ag_2. Section 2 describes our methodology of calculations while section 3 comprised results and discussion.

2. Method of calculations

The low-lying electronic configurations of Ag_3 and Au_3 can be rationalized as the Jahn–Teller components ($^2B_2$ and $^2A_1$) of the $^2E'$ electronic state arising from the D_{3h} equilateral triangular symmetry. Thus, we consider calculations of both the $^2B_2$ and $^2A_1$ surfaces as a function of bond lengths and angles.

We first carry out multi-configuration self-consistent field (MCSCF) calculations with the d shells of all the three atoms in the active space. MCSCF calculations were carried out using the complete active space MCSCF (CASSCF) method. In this method, the wavefunctions are constructed in the complete configuration space of strongly occupied orbitals of the separated atoms. The MCSCF calculations which we label d-CASSCF included the outer d and s orbitals and 33 outer electrons in the active space. The active space in the C_{2v} group consisted of 7 a_1 orbitals, 5 b_2 orbitals, 3 b_1 orbitals and 3 a_2 orbitals. The molecule was oriented on the yz plane with the z axis bisecting the M–M–M angle.

Relativistic effective core potentials with the outer $d^{10}s^1$ shells of the three atoms explicitly retained in the valence space were employed for both gold and silver. La John et al. [28] have generated Gaussian analytical fits for averaged relativistic potentials and spin–orbit operators for many elements. We employ these potentials together with the (3s2p4d) and (3s3p3d) basis sets shown in table 1. The d functions with largest exponents were contracted for silver.

Three types of configuration interaction (CI) calculations were carried out following CASSCF. The CI calculations carried out which we label SOCI (sec-

Table 1
Valence basis sets of Gaussian-type functions for Ag (3s2p4d/3s2p3d)

Atom	Shell	Exponential factor	Contract coefficient
Ag	s	0.4981	1.0
		0.1584	1.0
		0.0471	1.0
	p	0.0908	1.0
		0.0283	1.0
	d	2.4127	0.308853
		1.0153	0.450434
		0.4093	1.0
		0.1503	1.0

ond-order CI) were made following CASSCF and did not include the d electrons in the calculations. The SOCI calculations included (i) the configurations in the zeroth-order MCSCF, (ii) configurations generated by distributing 2 electrons in the MCSCF internal space and 1 electron in the orthogonal external space in all possible ways, and (iii) configurations generated by distributing 1 electron in the internal and 2 electrons in the external spaces in all possible ways. The objective of carrying out SOCI calculations with d shells frozen in the CI is to study the effect of d electron correlation corrections.

The CI calculations which included d correction effects to some degree are labeled d-POLCI. These calculations were carried out after d-CASSCF. The d-POLCI calculations included all 33 electrons and configurations in the CASSCF with coefficients $\geqslant 0.07$ as reference configurations. The POLCI configurations form a subset of MRSDCI (multireference singles+doubles) in which the configurations generated by distributing 2 electrons in the MCSCF-orthogonal space are omitted. The d-POLCI calculations thus included all single and most important double excitations from the various reference configurations.

The third set of calculations is labelled d-MRSDCI. These are the most accurate calculations carried out in this investigation. The d-MRSDCI calculations included all the 33 electrons, the configurations generated in the d-POLCI plus all the configurations generated by distributing the 2 electrons in the MCSCF-orthogonal (external) space from the leading reference configuration. The d-MRSDCI calculations thus include all possible single and double excitations from the leading configuration plus all possible single and most important double excitations from two other less important configurations. The d-MRSDCI calculations included about 400000 CSFS. The exact configuration counts of all the calculations carried out here are in table 2.

The importance of higher-order excitations not included in the MRSDCI was also studied using the Davidson correction method for higher-order unlinked cluster configurations. It was comforting to note that Davidson's correction did not change the actual energy separations by more than 0.07 kcal/mole for Au_3. Thus we believe that the present calculations on both clusters take into account the effects of electron correlations to a high order for a cluster containing 33 electrons.

The spin–orbit coupling effects could be important for Au_3. Although, to first order, the spin–orbit coupling effect would be zero for both Au_3 and Ag_3 primarily due to symmetry considerations, second-order off-diagonal spin–orbit matrix elements could be large for Au_3. Further, the existence of two low-lying electronic states for these clusters could lead to a considerable spin–orbit contamination. For Au_3, there could also be spin–orbit effects from the mixing of the 6p

Table 2
The dimensions of the configuration spaces in the CASSCF/POLCI/MRSDCI calculations of Au_3 and Ag_3

Species	State	CASSCF	SOCI	d-POLCI [a]	d-MRSDCI
Au_3	$^2A_1$	503	3760	33292	421140
Au_3	$^2B_2$	501	3700	38494	370689
Ag_3	$^2A_1$	503	3760	29685	365594
Ag_3	$^2B_2$	501	3700	38494	370689

[a] The d-POLCI calculations for the linear geometries included about 50000 configurations.

orbitals and fractional vacancies created in the nearly full d shells in higher-order CI. Thus we decided to investigate the spin–orbit effects for both the clusters.

The spin–orbit corrections were calculated using the recently developed relativistic configuration interaction method for polyatomics by one of the present authors (KB) [29]. The natural orbitals from the d-MRSDCI calculations were used as the orbital space for the relativistic configuration interactions. The spin–orbit operator was expressed as the difference of $l+\frac{1}{2}$ and $l-\frac{1}{2}$ relativistic effective potentials. The spin–orbit integrals were obtained using Pitzer's modified version of the ARGOS integral package to calculate these integrals. The relativistic configuration interaction calculations were carried out by adding the transformed spin–orbit integrals over the d-MRSDCI natural orbitals into the Hamiltonian matrix. Since the inclusion of the spin–orbit term into the Hamiltonian changes the symmetry group into a spin double group, all low-lying electronic configurations which have the same symmetry in the spin double group would mix in the relativistic CI. For Au_3 and Ag_3, both the $^2A_1$ and $^2B_2$ states correlated into the ^2E representation of the C_{2v}^2 group. The $^2A_1$ state with the open-shell spin α would mix with the $^2B_2$ state with the open-shell spin β. The relativistic CI calculations thus included the two leading configurations arising from the $^2A_1$ and $^2B_2$ states with α and β spins, respectively. The resulting state is labelled $^2A_1\alpha$ for convenience although it is a component of the ^2E state in the double group. Similarly calculations on the $^2B_2\alpha$ state were also carried out near the equilibrium geometry of the $^2B_2$ state. Another set of calculations with identical configurations without the spin–orbit matrix elements were also carried out. The difference between the two results was taken to be the effect of the spin–orbit term and was applied to the d-MRSDCI results.

The effect of d-correlation was also studied on Ag_2 and Au_2 by carrying out MRSDCI (multi-reference singles and doubles CI) calculations which allow excitations from d shells. The CASSCF wavefunction of the $^1\Sigma_g^+$ ground state of Ag_2 contains two configurations namely, $1\sigma_g^2$ and $1\sigma_u^2$. These two reference configurations were included in the MRSDCI calculations together with the d shells of the metal atoms. Single and double excitations from the $1\sigma_g$, $1\sigma_u$ and the d orbitals in the A_1 symmetry block were allowed in the MRSDCI calculations.

All calculations reported here were carried out using one of the author's (KB) [30] modified version of ALCHEMY II codes [31] to include relativistic effective core potentials as described in ref. [30].

3. Results and discussion

Tables 3 and 4 show the calculated geometries and energies of the low-lying electronic states of Ag_3 and Au_3, respectively. The d-POLCI results are the best of all calculations reported in these tables since these calculations include d correlation corrections. For Ag_3, the lowest state at all levels of calculations is the bent $^2B_2$ state. The $^2\Sigma_u^+$ state with a linear geometry as well as the $^2A_1$ state with an isosceles triangular geometry are close in energy to the $^2B_2$ state.

The ground state ($^2B_2$) of Ag_3 has an isosceles triangle structure with a near-equilateral apex angle of 63° at the POLCI level of calculations. Note that the d correlations change the apex angle and bond lengths substantially for the $^2B_2$ state. This aspect is discussed later. The Ag–Ag bond length of 2.76 Å although shorter than the corresponding CASSCF value, it appears to be somewhat long. The base of the isosceles triangle has a Ag–Ag bond length of 2.84 Å.

The gold trimer behaves similar to the silver trimer in that the ground state is a $^2B_2$ electronic state with an equilibrium geometry of an isosceles triangle with an apex angle of 63°. While the apex angles are almost the same for both Ag_3 and Au_3, the Au–Au bond lengths for the equal sides of the isosceles triangle are substantially shorter for Au_3. This shortening of 0.13–0.17 Å seen for all geometries and electronic states of Au_3 in comparison to Ag_3 is primarily attributed to relativistic mass–velocity contraction of the outer 6s orbital of the gold atom. This shortens the Au–Au bond and stabilizes the metal–metal bond in Au_3 in comparison to Ag_3.

The other interesting contrast between Ag_3 and Au_3 is that the $^2B_2$ and $^2A_1$ states are much closer in energy (0.67 kcal/mole) for Au_3 in comparison to Ag_3. In fact, at the d-CASSCF levels of calculation the $^2B_2$ is actually higher in energy in comparison to the $^2A_1$ state. The switching of the two electronic states is

Table 3
Geometries and energies of the electronic states of Ag_3 using various methods

State	d-CASSCF			SOCI			d-POLCI		
	geometry [a]		E [b]	geometry [a]		E [b]	geometry [a]		E [b]
	M_1–M_2 (Å)	θ (deg)		M_1–M_2 (Å)	θ (deg)		M_1–M_2 (Å)	θ (deg)	
$^2B_2$	2.84	102	0.0	2.82	104	0.0	2.76	63	0.0
$^2A_1$	3.26	50	2.85	3.09	52.8	0.58	2.85	56	2.36
$^2\Sigma_u^+$	2.87	180	0.24	2.82	180	0.82	2.77	180	4.59
$^2\Sigma_g^+$	3.25	180	19.08	3.06	180	22.30	3.01	180	26.65
Ag+Ag+Ag	7.50	180	20.96	7.50	180	32.50	7.50	180	34.70

[a] The two equal sides of the isosceles triangle; θ=apex angle.
[b] Zero energy for CASSCF is −111.81863 hartree; d-CASSCF is −111.81934; SOCI is −111.83787; d-POLCI is −111.84904. All energies are in kcal/mole with respect to the $^2B_2$ state.

caused by d correlation. For Ag_3 even at the CASSCF and d-CASSCF levels of theory the $^2B_2$ state is lower than the $^2A_1$ state.

The linear $^2\Sigma_u^+$ states of Au_3 and Ag_3 are about 4.4–4.6 kcal/mole above the $^2B_2$ bent state. Since this separation is small the M_3 (equilateral) $\rightleftharpoons M_3$ (isosceles) $\rightleftharpoons M_3$ (linear) interconversion is favorable in the $^2B_2$ surface.

Figs. 1 and 2 show the bending potential energy surfaces of Ag_3 and Au_3 obtained using POLCI calculations. As one can see from these figures the overall shapes of the two surfaces for Ag_3 and Au_3 are similar. The $^2B_2$ surface of Ag_3 is a bit shallow while that of Au_3 contains a deeper well near equilateral geometry. The $^2B_2$ surface of Au_3 has a saddlepoint which separates the linear and the bent geometry. For Ag_3, this surface is nearly flat in this region. The splitting of the linear–isosceles minima in the $^2B_2$ surface of Au_3 is smaller in comparison to Ag_3.

The $^2A_1$ bending surfaces of Au_3 and Ag_3 contain a bent minima (figs. 1 and 2). The linear $^2\Sigma_g^+$ geometry is much higher in energy for both the species. The saddlepoint in the $^2A_1$ surface is much higher in energy for Au_3 in comparison to Ag_3. Thus the interconversion of the triangular to linear geometry is facilitated only in the $^2B_2$ surface which does not possess a sharp barrier.

The atomization energy, that is, the energy for the $M_3(^2B_2) \rightarrow 3M(^2S)$ process is calculated to be 34.70 kcal/mole for Ag_3 while it is 62.28 kcal/mole for Au_3 at the POLCI level of theory. Thus Au_3 is much more stable with respect to the separated atoms in compar-

Table 4
Geometries and energies of the electronic states of Au_3 using various methods

State	d-CASSCF			SOCI			d-POLCI		
	geometry [a]		E [b]	geometry [a]		E [b]	geometry [a]		E [b]
	M_1–M_2 (Å)	θ (deg)		M_1–M_2 (Å)	θ (deg)		M_1–M_2 (Å)	θ (deg)	
$^2B_2$	2.67	70.8	1.85	–	–	–	2.63	63	0.0
$^2A_1$	2.76	57.6	2.98	2.84	55	0.63	2.73	56.6	0.67
$^2\Sigma_u^+$	2.66	180	0.0	2.65	180	0.0	2.60	180	4.35
$^2\Sigma_g^+$	2.76	180	26.76	2.75	180	28.13	2.63	180	29.23
Au+Au+Au	7.50	180	40.00	7.50	180	46.05	7.50	180	62.28

[a] Two equal sides of the isosceles triangle; θ=apex angle.
[b] Zero energy for CASSCF is −99.96191 hartree; d-CASSCF is −99.96538; SOCI is −99.97506; d-POLCI is −100.01199; d-POLCI energies are in kcal/mole with respect to the $^2B_2$ state, others are in kcal/mole with respect to the $^2\Sigma_u^+$ state.

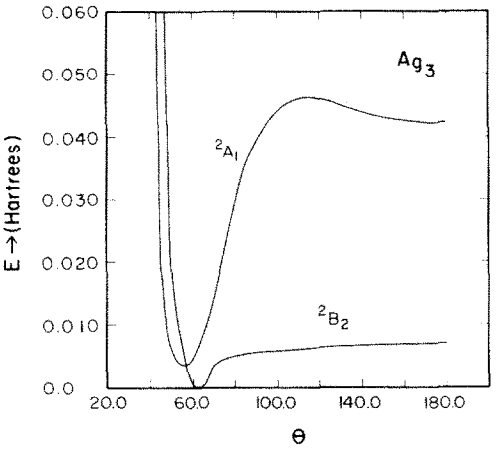

Fig. 1. The POLCI bending potential energy surfaces of the $^2A_1$ and $^2B_2$ states of Ag_3. The M–M bond distances (equal sides of the triangle) were optimized for all bending angles.

ison to Ag_3. This is primarily a consequence of relativistic effects which shrink the 6s orbitals of gold and thus stabilize the Au–Au bond in comparison to the Ag–Ag bond.

The dissociation energy D_e, that is, the energy for the process $M_3(^2B_2) \rightarrow M_2(^1\Sigma_g^+) + M(^2S)$ is calculated to be 0.67 and 0.74 for Ag_3 and Au_3, respectively at the SOCI level.

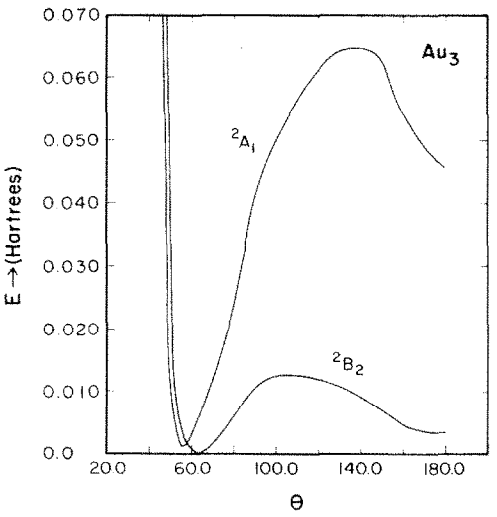

Fig. 2. The POLCI bending potential energy surfaces of the $^2A_1$ and $^2B_2$ states of Au_3. The M–M bond distances were optimized for all bending angles. Note that the splitting between the bent and linear minima of the $^2B_2$ surface for Au_3 is somewhat smaller than the corresponding minima for Ag_3.

Table 5
Geometries and energies of the electronic states of Au_2 and Ag_2

System	State	SOCI		d-MRSDCI	
		r (Å)	E (eV)	r (Å)	E (eV)
Ag_2	$^1\Sigma_g^+$	2.76	0.0 [a]	2.68	0.0
Ag+Ag		7.50	0.74	7.50	1.17
Au_2	$^1\Sigma_g^+$	2.60	0.0 [b]	2.56	0.0
Au+Au		7.50	1.26	7.50	1.68

[a] Zero energy for SOCI of Ag_2 is −74.55105 hartree; MRSDCI is −74.61903.

[b] Zero energy for SOCI of Au_2 is −66.64737 hartree. MRSDCI is −66.72898.

We also carried out CASSCF followed by SOCI and d-MRSDCI calculations on Ag_2 and Au_2. The results of our calculations for the dimers are shown in table 5. The d correlation corrections shorten the M–M bond by 0.08 and 0.04 Å for Ag_2 and Au_2, respectively. The D_e values are increased by 0.43 and 0.42 eV for Ag_2 and Au_2.

Since the $^2B_2$ and $^2A_1$ electronic states of both Ag_3 and Au_3 were close in energy we decided to carry out large-scale configuration interaction calculations with the objective of calculating the $^2B_2$–$^2A_1$ energy separations accurately for both the clusters. Table 6 shows the geometries and energy separations for both Ag_3 and Au_3 obtained using the d-MRSDCI method. As one can see from that table the bond lengths of the equal sides of the triangle do not change much due to higher-order correlation effects (0.01–0.04 Å) in comparison to the d-POLCI geometries. The apex angle of the triangle changes between 0.2 and 2.7°, the largest change being for the $^2B_2$ state. Even this

Table 6
MRSDCI geometries and energy separations of the electronic states of Au_3 and Ag_3 [a]

	State	R_e (Å)	θ_e (deg)	E (kcal/mole)
Au_3	$^2B_2$	2.60	65.7	0
Au_3	$^2A_1$	2.72	56.4	0.54 (0.61)
Ag_3	$^2B_2$	2.72	63.7	0
Ag_3	$^2A_1$	2.88	54.2	0.74

[a] The number in parentheses included the Davidson correction for higher-order unlinked cluster configurations not included in the MRSDCI.

change in angle when transpired into change in the bond length of the base of the triangle, is relatively small. Thus it is concluded that d-POLCI calculations yield geometries which are accurate to 4% of MRSDCI geometries. This is particularly important to know since we are carrying out calculations on tetramers of gold and silver for which MRSDCI calculations would be formidably difficult.

The MRSDCI $^2B_2$–$^2A_1$ energy separation of Au_3 decreases by only 0.13 kcal/mole in comparison to the d-POLCI separation. In fact, after Davidson's correction is introduced to the MRSDCI results, the $^2B_2$–$^2A_1$ separation almost becomes identical to the d-POLCI separation making us wonder if the large amounts of computer time spent on the large scale CI calculations which included about 400000 configurations was justified.

The d-MRSDCI $^2B_2$–$^2A_1$ energy splitting decreases by orders of magnitude for Ag_3 in comparison to the d-POLCI splitting. The d correlation effects are thus more significant for Ag_3 in comparison to Au_3. This is realized even upon inspection of the dimers of the two metal atoms. As one can see from table 5 more significant change in geometries and D_e values are brought about by d correlation effects for Ag_2 in comparison to Au_2 (cf. SOCI and d-MRSDCI results in table 5). Thus the d-MRSDCI calculations are more justifiable for Ag_3 in comparison to Au_3. Our calculated results for the bent electronic states of Ag_3 are in reasonable agreement with earlier single configuration SCF/CI treatment [36].

As mentioned in section 2, the spin–orbit effects could be important for both the clusters. The results of relativistic CI calculations which included the spin–orbit matrix elements in the Hamiltonian are shown in table 7. As one can see from table 7, the spin–orbit coupling reduces the $^2B_2$–$^2A_1$ energy separation to 0.16 kcal/mole. Although, in absolute magnitude this reduction corresponds to 0.38 kcal/mole in relative terms this is a reduction of 67% of the energy separation without the spin–orbit terms. Thus the spin–orbit effects are quite important for Au_3.

Table 7
The energy separations of the electronic states of Ag_3 and Au_3 including the spin–orbit effects.

	State	R_e (Å)	θ_e (deg)	E (kcal/mole)
Au_3	$^2B_2\alpha$	2.60	65.7	0
Au_3	$^2A_1\alpha$	2.72	56.4	0.16 (0.23)
Ag_3	$^2B_2\alpha$	2.72	63.7	0
Ag_3	$^2A_1\alpha$	2.88	54.2	0.69

The spin–orbit coupling reduces the $^2B_2$–$^2A_1$ energy separation by only 0.05 kcal/mole for Ag_3. Thus for Ag_3 the spin–orbit effects are less important but correlation effects are more important. For the gold trimer, the converse is true.

The relative importance of correlation versus spin–orbit interaction can be assessed qualitatively by analyzing the atomic energy levels [32] of the silver and gold atoms. The spin–orbit splitting of the ^2D state into $^2D_{5/2}$ and $^2D_{3/2}$ ($5d^96s^2$) is 12274 cm^{-1} for gold. The corresponding splitting for silver is only 4472 cm^{-1}. Similarly, the splitting of the ^2P state which arises from the outer $d^{10}p^1$ configuration into $^2P_{1/2}$ and $^2P_{3/2}$ states for gold and silver atoms are 3815 and 200 cm^{-1}, respectively. Thus spin–orbit effects are dramatically larger for gold in comparison to silver.

Next, we compare our calculational results with available experimental data on these species. ESR spectra of both Ag_3 and Au_3 have been investigated by many workers [7,9,10,33]. Many of the experimental investigations on the coinage metal polyatomics have been reviewed in refs. [10,34]. The Raman spectra of Ag_3 have been recorded by Schulze et al. [4] while optical spectra of both Ag_3 and Au_3 have been recorded by Ozin and co-workers [6,35].

The ESR spectra of both silver and gold trimers appear to reveal that the ground state of these species is a $^2B_2$ electronic state with a bent geometry. All the ESR investigations reveal a bent structure for Ag_3 seriously questioning the linear structure proposed by Schulze et al. [4]. Our CAS/MRSDCI calculations on Ag_3 also yield a bent $^2B_2$ state, the linear $^2\Sigma_u^+$ state being at least 5 kcal/mole above the bent state. However, all of the ESR investigations have been carried out in rare gas matrices which seem to favor an obtuse triangle geometry contradicting the acute triangular structure predicted by the most accurate CASSCF/MRSDCI calculations. As one can see from fig. 1, the potential energy surface of the $^2B_2$ state is somewhat flat in the obtuse angle region. Since the change in the energies in this region is little, the matrix may favor an obtuse triangular structure. It seems that gas phase spectroscopic investigations are war-

ranted to yield accurate geometries for the $^2B_2$ state to compare with our calculational results.

Note that separations between the two Jahn–Teller components of the $^2E'$ state (D_{3h}) are very small for both the trimers. This small energy difference is consistent with the isomerization effects discussed by Ozin, Huber and Mitchell [6].

The ESR investigations of both Ag_3 and Au_3 [9,33] have revealed that the spin population of the unpaired electron is predominantly 5s and 6s orbitals of the side atoms than the central atom. In C_{2v} symmetry, if the unpaired electron is in the b_2 orbital which leads to a $^2B_2$ state then the s orbital of the central atom cannot contribute to the open-shell orbital due to symmetry considerations. For Au_3, the 6s unpaired spin population was found from hyperfine interactions [33] to be about 84% on the terminal atom. The natural orbitals constructed from our CASSCF/MRSDCI calculations on Au_3 agree with this finding in that the $1b_2$ orbital is predominantly made of the 6s orbitals of the base atoms of the isosceles triangle although both the 6p and 5d orbitals of both the apex and base atoms make non-negligible contribution to the nearly singly occupied (density=0.9929) b_2 orbital of Au_3. The open-shell b_2 natural orbital of Ag_3 which has a density of 0.9893 has a slightly less s character in comparison to Au_3; the 5p and 4d orbitals of both the apex and base atoms make greater contribution in comparison to Au_3. Thus all the results agree with the populations obtained from the experimental hyperfine structure.

The optical spectra of Au_3 recorded by Klotzbücher and Ozin [35] have revealed two bands for Au_3 in the region of 34246 and 21231 cm^{-1}. These bands have not yet been assigned unambiguously. We propose to extend the present calculations on Au_3 to other excited states of Au_3 with the objective of assigning these transitions.

Table 8 shows the dipole moments of the low-lying electronic states of both the gold and silver clusters using the d-MRSDCI natural orbitals. These dipole moments should be accurate to within 10%. The comparison of the dipole moments of gold and silver trimers reveals that the gold trimer is more ionic than the silver trimer. Note that the gold trimer has shorter M–M bond lengths in comparison to the silver trimer. Thus larger dipole moments for Au_3 in comparison to Ag_3 should imply a considerable increase in the charges for Au_3.

Table 8
Dipole moments of the low-lying electronic states of Ag_3 and Au_3 calculated using the MRSDCI calculation

	State	μ [a] (D)
Au_3	$^2B_2$	1.492
Au_3	$^2A_1$	−1.871
Ag_3	$^2B_2$	0.954
Ag_3	$^2A_1$	−1.791

[a] Positive polarity implies that the apex atom of the isosceles triangle carries the positive charge.

The relative signs of the calculated dipole moments of the two Jahn–Teller components of the gold and silver clusters are also quite interesting. In the $^2B_2$ state the apex atom of the isosceles triangle carries the positive charge while in the $^2A_1$ state the apex atom carries the negative charge. The opposite signs of the two dipole moments are consistent with the fact that for the $^2E'$ state (equilateral triangle) the dipole moment should be zero. Thus the Jahn–Teller distortion should change the dipole moments of the two components in the opposite direction (center of gravity rule). However, the dramatic change from the zero value of the dipole moment is certainly interesting since the geometries of the two states are not very far from being an equilateral triangle.

Table 9 shows the Mulliken population analyses of the d-MRSDCI natural orbitals Au_3 and Ag_3. The ALCHEMY codes which we use, carry out population analysis on a basis set of six component d orbitals and includes the $d_{x^2+y^2+z^2}$ component which should actually be added to the s population. One of the authors (KB) developed a code to project the $x^2+y^2+z^2$ component of the d orbitals and extract the corresponding population and add it to the s populations. Table 9 reports the corrected d and s populations. In comparing the populations of the clusters the striking contrast is that the overall p population is 0.29 e lower in Au_3 in comparison to Ag_3. This is accompanied by an increase in the s populations in Au_3 in comparison to Ag_3. Thus the participation of the next p shell is less in Au_3 in comparison to Ag_3. This can be explained based on the atomic states of Ag and Au. For Ag the first excited state arises from the $4d^{10}5p$ configuration which is about 30000 cm^{-1}

Table 9
Mulliken population analysis for Au_3 and Ag_3 [a]

	State	Gross								Overlap [b]
		M	M_2	M(s)	M_2(s)	M(p)	M_2(p)	M(d)	M_2(d)	
Au_3	$^2B_2$	10.84	22.16	0.741	2.167	0.147	0.226	9.950	19.769	0.608
	$^2\Sigma_u^+$	11.32	21.68	1.178	1.808	0.119	0.010	10.025	19.859	0.632
	$^2A_1$	11.14	21.86	1.143	1.802	0.109	0.261	9.885	19.800	0.114
	$^2\Sigma_g^+$	11.16	21.84	0.849	1.859	0.313	0.016	9.999	19.964	0.512
Ag_3	$^2B_2$	10.81	22.19	0.602	1.838	0.227	0.438	9.979	19.917	0.812
	$^2\Sigma_u^+$	11.17	21.83	1.004	1.815	0.160	0.060	10.005	19.955	0.867
	$^2A_1$	11.09	21.91	0.971	1.607	0.167	0.386	9.950	19.918	0.572
	$^2\Sigma_g^+$	11.15	21.85	0.787	1.783	0.359	0.101	10.005	19.964	0.661

[a] M_2 refers to the two equivalent atoms of the cluster. [b] Total overlap of the central atom with the two side atoms.

above the ground state [32]. The $4d^95s^2$ ($^2D_{5/2,3/2}$) states are about 30300–35000 cm^{-1} above the ground state. Thus the participation of the 5p orbital is more important than the 4d orbital for silver. For gold however, the lowest excited states arise from the $5d^96s^2$ configuration ($^2D_{5/2}$, 9161 cm^{-1}, $^2D_{3/2}$, 21435 cm^{-1}). The $5d^{10}6p$ configuration is about 40000 cm^{-1} above the ground state ^2S atom. Thus the participation of the 5d orbital for gold is more important than the 6p orbital.

The importance of the 5d participation in Au_3 is also reflected by the fact that the $^2B_2$ state does not

Table 10
d-POLCI wavefunction of the low-lying states of Ag_3

Coefficients	Configuration																		
	$1a_1$	$2a_1$	$3a_1$	$4a_1$	$5a_1$	$6a_1$	$7a_1$	$8a_1$	$1b_2$	$2b_2$	$3b_2$	$4b_2$	$5b_2$	$1b_1$	$2b_1$	$3b_1$	$1a_2$	$2a_2$	$3a_2$
$^2B_2$ ($\theta=63°$)																			
0.963	2	2	2	2	2	2	0	0	2	2	2	2	1	2	2	2	2	2	2
0.108	2	2	2	2	2	1	1	0	2	2	2	2	1	2	2	2	2	2	2
−0.088	2	2	2	2	2	0	2	0	2	2	2	2	1	2	2	2	2	2	2
$^2A_1$ ($\theta=56°$)																			
−0.960	2	2	2	2	2	2	1	0	2	2	2	2	0	2	2	2	2	2	2
0.113	2	2	2	2	2	0	1	0	2	2	2	2	2	2	2	2	2	2	2
0.083	2	2	2	2	2	1	1	1	2	2	2	2	0	2	2	2	2	2	2
$^2A_1$ ($\theta=120°$)																			
−0.723	2	2	2	2	2	1	0	0	2	2	2	2	2	2	2	2	2	2	2
−0.588	2	2	2	2	2	2	1	0	2	2	2	2	0	2	2	2	2	2	2
0.257	2	2	2	2	2	1	2	0	2	2	2	2	0	2	2	2	2	2	2
0.200	2	2	2	2	2	0	1	0	2	2	2	2	2	2	2	2	2	2	2
$^2A_1$ ($\theta=180°$)																			
0.856	2	2	2	2	2	1	0	0	2	2	2	2	2	2	2	2	2	2	2
0.406	2	2	2	2	2	2	1	0	2	2	2	2	0	2	2	2	2	2	2
−0.245	2	2	2	2	2	1	2	0	2	2	2	2	0	2	2	2	2	2	2
−0.103	2	2	2	2	2	0	1	0	2	2	2	2	0	2	2	2	2	2	2

Table 11
d-POLCI wavefunction of the low-lying states of Au_3

Coefficients	Configuration																	
	$1a_1$	$2a_1$	$3a_1$	$4a_1$	$5a_1$	$6a_1$	$7a_1$	$1b_2$	$2b_2$	$3b_2$	$4b_2$	$5b_2$	$1b_1$	$2b_1$	$3b_1$	$1a_2$	$2a_2$	$3a_2$
$^2B_2$ ($\theta=63°$)																		
0.958	2	2	2	2	2	2	0	2	2	2	2	1	2	2	2	2	2	2
0.076	2	2	2	2	2	1	1	2	2	2	2	1	2	2	2	2	2	2
−0.070	2	2	2	2	2	0	2	2	2	2	2	1	2	2	2	2	2	2
$^2A_1$ ($\theta=56.6°$)																		
0.957	2	2	2	2	2	2	1	2	2	2	2	0	2	2	2	2	2	2
−0.084	2	2	2	2	2	0	1	2	2	2	2	2	2	2	2	2	2	2
−0.082	2	2	2	2	2	2	1	1	2	2	2	1	2	2	2	2	2	2
0.081	2	2	2	2	2	2	1	2	2	2	1	1	2	2	2	2	2	2
$^2A_1$ ($\theta=120°$)																		
0.760	2	2	2	2	2	1	0	2	2	2	2	2	2	2	2	2	2	2
−0.525	2	2	2	2	2	2	1	2	2	2	2	0	2	2	2	2	2	2
−0.199	2	2	2	2	1	2	0	2	2	2	2	2	2	2	2	2	2	2
−0.173	2	2	2	2	2	1	2	2	2	2	2	0	2	2	2	2	2	2
−0.087	2	2	2	2	2	2	1	2	2	2	1	1	2	2	2	2	2	2
0.080	2	2	2	2	2	0	1	2	2	2	2	2	2	2	2	2	2	2
$^2A_1$ ($\theta=180°$)																		
0.904	2	2	2	2	2	1	0	2	2	2	2	2	2	2	2	2	2	2
−0.252	2	2	2	2	2	2	1	2	2	2	2	0	2	2	2	2	2	2
−0.152	2	2	2	2	2	1	2	2	2	2	2	0	2	2	2	2	2	2
0.133	2	2	2	2	1	2	0	2	2	2	2	2	2	2	2	2	2	2
−0.097	2	2	2	2	1	1	1	2	2	2	2	2	2	2	2	2	2	2
0.085	2	2	2	2	2	2	1	2	2	2	1	1	2	2	2	2	2	2

form an appreciable bond (bent) if d correlation is not allowed. The d correlation effects change the bond angle substantially in Au_3 for the $^2B_2$ state since the $5d^96s^2$ configuration plays an important role in the $^2B_2$ state.

The leading configurations of the d-POLCI wavefunctions of the two states ($^2B_2$ and $^2A_1$) for both Ag_3 and Au_3 are shown in tables 10 and 11, respectively. The comparison shows that the leading configuration has a slightly larger coefficient for Ag_3 for the $^2A_1$ and $^2B_2$ bent states. The CI wavefunction at the saddle-point of the $^2A_1$ state for both Au_3 and Ag_3 is quite mixed with 4 configurations indicating that the barrier heights for both the systems could be lowered by higher-order correlations. The leading configuration of the d-POLCI wavefunction of Au_3 has a coefficient of 0.958 and 0.957 respectively for the $^2B_2$ and $^2A_1$ states. The corresponding coefficients for Ag_3 are 0.963 and 0.960, respectively.

Table 12 shows the nature of the relativistic CI wavefunctions for the two lowest states of Ag_3 and Au_3. The mixing of the $^2A_1$ state (with α spin) with the $^2B_2$ state (with β spin) is certainly of considerable interest since this mixing is brought about primarily through the spin–orbit coupling term. As can be seen from table 12, the spin–orbit contamination in the $^2A_1\alpha$ state is about 1% while it is 0.6% in the

Table 12
The effect of spin–orbit contamination. The weights of different electronic states in the RCI wavefunction

		Percentage of contribution
Au_3	$^2A_1\alpha$	$^2A_1$ (92), $^2B_2$ (1)
Au_3	$^2B_2\alpha$	$^2B_2$ (93), $^2A_1$ (0.6)
Ag_3	$^2A_1\alpha$	$^2A_1$ (93), $^2B_2$ (0.02)
Ag_3	$^2B_2\alpha$	$^2B_2$ (94), $^2A_1$ (0.0014)

$^2B_2\alpha$ state for Au_3. For Ag_3 this contamination is orders of magnitude lower (0.02%, 0.001%). Thus the spin–orbit contamination is negligible for Ag_3 but small for Au_3. It is also of interest to note that the $^2A_1\alpha$ and $^2B_2\beta$ with opposite signs characterize the $^2E_{1/2}$ and $^2E_{3/2}$ components in the double group. The sign of the $^2B_2\beta$ configuration is thus imaginary.

4. Conclusion

In this investigation, CASSCF/SOCI, d-CASSCF/d-POLCI, d-CASSCF/d-MRSDCI calculations were carried out on the $^2B_2$ and $^2A_1$ electronic states of Ag_3 and Au_3 with all the 33 electrons in the active space. For both the clusters the $^2B_2$ state was found to be the lowest with an isosceles triangular structure and an acute apex angle of 65.7° for Au_3 and 63.7° for Ag_3. The $^2A_1$ electronic state also has an acute isosceles triangular geometry (apex angle 56.4° for Au_3, 54.2° for Ag_3). The $^2B_2$–$^2A_1$ energy separations including spin–orbit effects are 0.16 kcal/mole for Au_3 and 0.69 kcal/mole for Ag_3. The spin–orbit effects were found to be more important for Au_3 whereas correlation effects are found to be more important for Ag_3. The bending potential energy surfaces of both the $^2A_1$ and $^2B_2$ states were obtained at the d-POLCI level. The $^2B_2$ surface was found to be shallow while the $^2A_1$ surface has a large barrier in passing from near-equilateral to linear geometry. The atomization energies of Au_3 and Ag_3 at the d-POLCI level of theory are 34.7 and 62.28 kcal/mole, respectively. The D_e values for Ag_3 and Au_3 are calculated to be 15.5 and 17.1 kcal/mole, respectively. The Mulliken population analyses of these two clusters reveal that for Ag_3 the participation of the 5p orbital is more important than the corresponding participation of the 6p orbital in Au_3. The 5d orbital plays a slightly more important role in Au_3 than the corresponding 4d orbital for Ag_3. The $^2B_2$ and $^2A_1$ electronic states are ionic for both Au_3 and Ag_3 but the electronic states of Au_3 are more ionic than Ag_3. The dipole moments of the two Jahn–Teller components are large and opposite in signs. The relativistic mass velocity contraction of the outer 6s orbital of the gold atom leads to a shorter and more stable M–M bound in the gold trimer in comparison to the silver trimer.

Acknowledgement

This research was supported by the US Department of Energy under grant DE-FG02-86ER-13558. The authors thank Dr. PingYi Feng for her help in MRSDCI calculations.

References

[1] R.C. Batezold and J.F. Hamilton, Progr. Solid State Chem. 15 (1983) 1.
[2] S.C. Davis and K.J. Klabunde, Chem. Rev. 82 (1982) 153.
[3] M. Morse, Chem. Rev. 86 (1986) 1049.
[4] W. Schulze, H.U. Becker, R. Minkwitz and K. Manzel, Chem. Phys. Letters 55 (1978) 59.
[5] M. Moskovits and G.A. Ozin, J. Phys. Chem. 72 (1980) 2267.
[6] G.A. Ozin, H. Huber and S.A. Mitchell, Inorg. Chem. 18 (1979) 2932.
[7] W.E. Klotzbücher and G.A. Ozin, Inorg. Chem. 19 (1980) 3767.
[8] K. Hilpert and K.A. Gingerich, Ber. Bunsenges. Physik. Chem. 84 (1980) 739.
[9] J.A. Howard, K.F. Preston and B. Mile, J. Am. Chem. Soc. 103 (1981) 6226.
[10] J.A. Howard, R. Sutcliffe and B. Mile, Surface Sci. 156 (1985) 214.
[11] R.C. Baetzold, J. Chem. Phys. 55 (1971) 4363.
[12] R.C. Baetzold, J. Chem. Phys. 68 (1978) 555.
[13] S.C. Richtsmeier, J.L. Gole and D.A. Dixon, Proc. Natl. Acad. Sci. US 77 (1980) 5611.
[14] S.C. Richtsmeier, R.A. Eades, D.A. Dixon and J.L. Gold, Am. Chem. Soc. Symp. Ser. No. 179 (1982) 178.
[15] H. Basch, J. Am. Chem. Soc. 103 (1981) 4657.
[16] Y.S. Lee, W.C. Ermler and K.S. Pitzer, J. Chem. Phys. 73 (1980) 360.
[17] Y.S. Lee, W.C. Ermler and K.S. Pitzer, J. Chem. Phys. 70 (1979) 288.
[18] K. Balasubramanian and M.Z. Liao, J. Chem. Phys. 86 (1987) 5587.
[19] K.S. Pitzer, Intern. J. Quantum Chem. 23 (1984) 131.
[20] K.S. Pitzer, Accounts Chem. Res. 12 (1979) 271.
[21] K. Balasubramanian and K.S. Pitzer, Advan. Chem. Phys. 67 (1987) 287.
[22] K. Balasubramanian, J. Chem. Phys. 85 (1986) 1443.
[23] K. Balasubramanian, Chem. Phys. Letters 111 (1985) 201.
[24] K. Balasubramanian, J. Chem. Phys. 85 (1986) 3401.
[25] K. Balasubramanian, J. Chem. Phys. 82 (1985) 3741.
[26] K. Balasubramanian, Chem. Phys. Letters 127 (1986) 324.
[27] K. Balasubramanian, Chem. Phys. Letters 125 (1986) 400.
[28] L.A. LaJohn, P.A. Christiansen, R.B. Ross, T. Atashroo and W.C. Ermler, J. Chem. Phys. 87 (1987) 2812.
[29] K. Balasubramanian, J. Chem. Phys., to be published.
[30] K. Balasubramanian, Chem. Phys. Letters 127 (1986) 585.

[31] B. Liu, M. Yoshimine and B. Lengsfield, ALCHEMY II Codes.

[32] C.E. Moore, Atomic energy levels (Natl. Bur. Stds., Washington, 1971).

[33] J.A. Howard, R. Sutcliffe and B. Mile, J. Chem. Soc. Chem. Commun. (1983) 1449.

[34] W. Weltner Jr. and R.J. van Zee, Ann. Rev. Phys. Chem. (1984) 291.

[35] W.G. Klotzbücher and G. Ozin, Inorg. Chem. 19 (1980) 3767.

[36] S.P. Walch, C.W. Bauschlicher Jr. and S.R. Langhoff, J. Chem. Phys. 85 (1986) 5900.